Fuzzy Sets and Systems 50 (1992) 15–34
North-Holland

Fuzzy Medial Axis Transformation (FMAT): Practical feasibility

Sankar K. Pal* and Lui Wang
National Aeronautics & Space Administration, Lyndon B. Johnson Space Center, Houston, TX, USA

Received April 1991
Revised July 1991

Abstract: The Fuzzy Medial Axis Transformation (FMAT) of a fuzzy set f is a set of fuzzy disks whose sup is f. Unfortunately, specifying the FMAT sometimes requires more storage space than specifying f itself. The present paper describes some techniques to improve the compact representation of FMAT; thereby making it practically feasible and useful. The algorithms involve reduction of redundancy in FMAT, its approximation, and reduction of the searching spaces for its computation. The computational aspects for the convenience of writing an efficient program have also been described. A concept of 'sponsoring capability' of a pixel is described in order to view the principle of removing redundancy in FMAT and to generate its approximation. Two kinds of approximations are made, namely, distributed approximation and optimum fuzzy compactness. The aforesaid features have been demonstrated on a gray image.

Keywords: Fuzzy Medial Axis Transformation (FMAT); fuzzy disk; fuzzy geometry; image processing/representation.

1. Introduction

The problem of extracting the Medial Axis Transformation (MAT) plays a key role in the field of image processing, analysis and recognition because of the simplicity of image (and hence object) representation and skeleton extraction it allows. There has been an extensive research done [12] in extracting the medial axis of a region and skeleton of elongated objects from a two tone image.

Correspondence to: S.K. Pal, Software Technology Branch/PT4, National Aeronautics & Space Administration, Lyndon B. Johnson Space Center, Houston, TX 77058, USA.

* On leave from the Eleetronics & Communication Sciences Unit, Indian Statistical Institute, Calcutta, India.

The Medial Axis (MA) of a subset S of a binary picture is the set of those points in S whose distances from $\bar{S}$ (complement of S) are local maxima. The distance of a point P in S from $\bar{S}$ is the length of a shortest path from P to $\bar{S}$. The MAT of S consists of the aforesaid local maxima points together with their distances from $\bar{S}$. It provides a compact (economical) representation of S so that S can be reconstructed from its MAT. The MA of S can be regarded as a generalized axis of its symmetry and constitutes also a kind of skeleton, if S is elongated. Note that the word 'kind of' is used to mean that such a skeleton may be disconnected, since the MA is a union of the local maxima points.

From the aforesaid definitions it is seen that the MAT of a region in a binary picture is determined with respect to its boundary. In a gray tone image, the boundaries among various regions are not well defined. A few generalizations of MAT have been proposed in order to make them applicable to gray tone images. These include SPAN (Spatial Piecewise Approximation by Neighborhoods) [1], GRAYMAT [2] and MMMAT [10]. SPAN [1] provides an approximated representation of an image in terms of centers, radii and average gray level of homogeneous disks. GRAYMAT [2] is based on the concept of gray-weighted distance of a point from the background and therefore it requires an image be segmented into zeros (background) and non-zeros (object). MMMAT [10] is based on iterative min and max operations, and does not require the picture to be segmented. However, the number of iterations depends on the application and the border effects become a serious problem when the local min operation is iterated several times. All these techniques reduce to the MAT in the case of a two-tone image. They provide a reasonable gray medial axis (and skeleton) for the darker pixels in the case of gray tone image but, the original (input)

gray image, in any case, can not be reconstructed from its MMMAT or SPAN or GRAYMAT values. This property of image reconstruction is supposed to be an important characteristic of the MAT representation. Furthermore, the requirement of an image to be segmented into zero (background) and non-zero (object) needs the selection of threshold be made judiciously because the resulting skeleton is dependent on that selection.

There have also been some attempts made for extracting a gray skeleton of an image, but without using the concept of MAT. These include the fuzzy skeletonization technique [3] and the ridge seeking method [13]. Fuzzy skeletonization [3] needs an initial fuzzy segmentation of the image space so that the membership of a pixel for the subset skeleton can be computed with respect to the ε edge (edge points of object after which its class membership value is less than or equal to ε, $0 < \varepsilon \leq 1$) of the object region. The ridge seeking [13] method also requires that the pixels with gray value below a certain threshold to be set to zero. The skeletons produced by these methods do not depend much on the boundary selection. Since these techniques are not formulated from the point of MAT construction, the question of reconstruction of original gray image did not get any attention.

A Fuzzy Medial Axis Transformation (FMAT) based on the concept of fuzzy disks has recently been defined by Pal and Rosenfeld [9] by making a straightforward generalization of the MAT definition to the fuzzy subsets of a metric space. A *fuzzy disk* g_P centered at a point P is a fuzzy set in which membership value depends only on the distance from P. Since the gray level (scaled in $[0, 1]$) of a pixel can be regarded as its degree of membership in the set of high-valued ('bright') pixels, a gray scale can be regarded as a fuzzy set.

Unfortunately, for a gray image X, specifying the FMAT may require more storage space than specifying the image itself. The FMAT is seen to be redundant in the sense of representation and reconstruction of X. Moreover, its computational aspects were not addressed in [9]. In fact, it is found to be very expensive if one needs to check the inclusion (subset) condition of a fuzzy disk g_P by another disk g_Q for all the points in an image.

The present work describes some algorithms on those issues. The problem of reducing redundancy is tackled by selecting a set of fuzzy disks which together contain a fuzzy disk g_P for its deletion from the medial axis (MA) output. The computational algorithm developed in this context is based on the concept of 'sponsoring' capability of a pixel and it involves the process of successive deletion of pixels from exterior to interior of the image. The algorithm can also be used for two tone (binary) images. Three different techniques have then been developed to provide approximated FMAT versions so that the image representation becomes economical without affecting much of its reconstruction and it also provides good skeletons of the object regions (darker pixels). A set of criteria is finally established which allows one to work with a much smaller subset of an image space and therefore reduces significantly the time of computation of FMAT. Their graphical representation has also been provided to facilitate the task of programming. The performance of the algorithms is demonstrated on a gray image.

Section 2 describes the distance measures d_4 and d_8 in a digital picture, the definition of MAT of a binary (or crisp) image and its various characteristics for the convenience of understanding the FMAT of a gray image. The definition of FMAT [9] and some remarks on it are given in Section 3. Section 4 explains the redundancy removal techniques. The methods of reducing the searching space and the time of computation are explained in Section 5. Various approximation techniques are described in Section 6. Section 7 demonstrates the experimental results.

2. Medial Axis Transformation (MAT)

2.1. *Distance measures* [12]

Let X be a digital picture (image) of size $M \times N$. The city block distance between two points $P(x, y)$ and $Q(u, v)$, $x, u = 0, 1, 2, \ldots, M-1$; $y, v = 0, 1, 2, \ldots, N-1$, in a digital picture is defined as

$$d_4(P, Q) = |x - u| + |y - v|. \tag{1}$$

The chessboard distance between them is

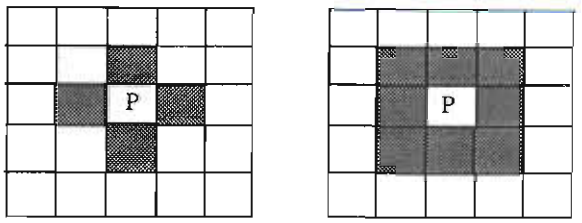

Fig. 1. Disks corresponding to $d_4 = 1$ and $d_8 = 1$.

defined as

$$d_8(P, Q) = \max(|x - u|, |y - v|). \quad (2)$$

These measures satisfy the metric properties and are simpler than the Euclidean distance to work on a digital image.

Points at a city block distance $d_4 = 1$ and $d_8 = 1$ from P respectively represent 4-neighbors and 8-neighbors of P. The points at a chessboard distance $d_4 \leq r$ from P form a diamond (i.e., diagonally oriented square) centered at P. Similarly, the points at $d_8 \leq r$ from P form an upright square of odd side length centered at P. These are shown in Figure 1 when $M = N = 5$ and $r = 1$. Let us call them diamond disk and upright square disk of radius 1. The distance between a point P and a set S is defined to be the shortest distance between P and any point of S.

2.2. Medial axis transform of a binary (two-tone) image

Let X be a binary (two-tone) image i.e., each point in X can have a value either 0 or 1. In the previous section it is seen that the points within a given chessboard distance (d_8) of P form an upright square of odd side length centered at P. Let us associate with each point $P \in X$ a set of such upright squares of constant value. (Though a set of upright squares formed by chessboard distance is considered here, the discussion may be generalized to any family of mutually similar shapes formed by other distance measures.) For every point P, let D_P be the largest square (or disk) that is contained in X and has a constant value v_P. Let r_P be the radius of D_P. Then X is the union of the D_P's. Let C be a subset of X such that, for all $P \in X$, there exists $Q \in C$ so that $D_Q \supseteq D_P$. (In other words, C is a set of points Q at which D_Q is a local maximum i.e., for any neighbor P of Q, $D_Q \supseteq D_P$.) We call C a sufficient subset of X. Evidently, for any such C, X is the union of the D_Q's, $Q \in C$.

The image X can therefore be completely represented by the centers P, radii r_P and values v_P of the disks D_P, $P \in C$, because any point of X must lie in at least one of these disks (blocks). The set C is called the medial axis (or symmetric axis) of X, and the set of D_P's, i.e., the set of all P, r_P and v_P for $P \in C$, is called the Medial Axis Transformation of X.

Figures 2 and 3(a) show the MAT representations of two binary pictures of sizes 8×8 and 5×8 using upright square disks. The centers of maximal blocks with valne $v = 1$ are underlined. The center coordinates (x, y) and radii of the maximal blocks are shown considering that the lower left corner of the images has coordinate $(1, 1)$. The images can therefore be reconstructed once the values of (x, y), r and v of the maximal blocks are given.

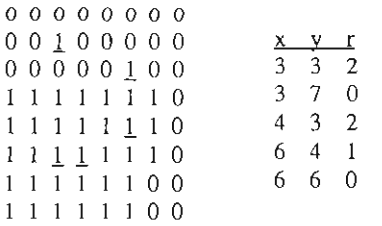

Fig. 2. MAT representation of an 8×8 binary image [12].

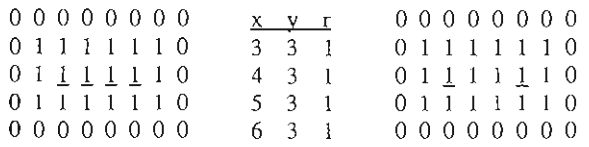

(a) (b)

Fig. 3. (a) MAT representation of a 5×8 binary image. (b) MAT after removing redundancy.

2.3. Some remarks

(i) Note that for the binary images (Figures 2 and 3), one needs to specify the maximal blocks of only one value (of 1's). The points not covered by these blocks must have the value of 0's.

If X is an L-level image, i.e., each point in X can take a value from $\{0, 1, 2, \ldots, L-1\}$, then

0	0	0	0	0	0	0	0
0	0	1	0	0	0	0	0
0	0	0	0	0	1	0	0
1	1	1	1	1	1	1	0
1	2	2	2	2	2	1	0
1	2	3	3	2	1	1	0
1	2	2	2	2	1	0	0
1	1	1	1	1	1	0	0

(a)

0	0	0	0	0	0	0	0
0	0	1	0	0	0	0	0
0	0	0	0	0	1	0	0
1	1	1	1	1	2	1	0
1	2	2	2	2	2	1	0
1	2	3	3	3	2	1	0
1	2	2	2	2	1	0	0
1	1	1	1	1	1	0	0

(b)

Fig. 4. Distanee to $\bar{R}$, the MA (local maxima) points are underlined. (a) Using d_8-metric. (h) Using d_4-metric.

X can be viewed as consisting of L constant-valued regions. In that case, one needs to specify the maximal blocks for $L-1$ of the values; the points not covered by any of the maximal blocks must have the omitted value.

(ii) The MAT representation may still be redundant in the sense of reconstruction of image, i.e., some blocks (disks) may be contained in unions of others. For example, the disks $D(4, 3)$ and $D(5, 3)$ at the points $(4, 3)$ and $(5, 3)$ of Figure 3(a) are redundant, because these are contained in the union set $(D(3, 3) \cup D(6, 3))$. If these are removed (as shown in Figure 3(b)), one can still reconstruct the image. However, there does not seem to be any simple way of reducting this redundancy without carrying out a lengthy search process.

(iii) When X is considered to be partitioned into R and $\bar{R}$ (i.e., object and background, say) the medial axis of R may be viewed as consisting of only those points of R whose distances from $\bar{R}$ are local maximum. If d_8 is used as the metric, local maximum means that no 8-neighbors of the point has greater distance from $\bar{R}$. This is explained in Figure 4(a) when the regions of 1's in Figure 2 are considered as R and that of 0's as $\bar{R}$. The entries denote the d_8-values of pixels from $\bar{R}$.

Similarly, if one uses city block distance (d_4) for obtaining a MAT of R, the local maxima then refer to 4-neighbors. The corresponding d_4-values and the medial axis thus obtained are shown in Figure 4(b). The MAT operation is therefore seen to be influenced by the choice of a distance measure.

(iv) The concept of 'maximal block' or 'local distance maxima' makes the centers of the MAT located at mid points or along local symmetry axis of the regions of constant value in X. For example, if we consider the point $P(5, 2)$ as an MA point instead of $P(6, 4)$ in Figure 4(a) (or consider the point $P(7, 4)$ instead of $P(6, 4)$ in Figure 4(b)), the changed MAT will still be able to represent and to reconstruct the image of Figure 2 with the bit requirement the same as before. Note that the disks centered at the replacing points $(5, 2)$ and $(7, 4)$ are not maximal (or their distances from the border are not local maxima) and therefore selection of these disks make the MA located off-center from the uniform region.

(v) Since the MA is the set of local maxima of the distances to $\bar{R}$, it is usually disconnected, and it is two-pixel thick at the places where the region R has even width. These factors are to be taken care of while extracting the skeleton of an elongated region R using its MAT.

3. Fuzzy Medial Axis Transformation (FMAT) [9]

Let D be a metric space with metric d and let f be a fuzzy subset of D. For each $P \in D$, let g_P^f be the fuzzy subset of D with membership at each point $Q \in D$ defined by

$$g_P^f(Q) = \inf_{d(P,R)=d(P,Q)} f(R), \tag{3}$$

with $f(R)$ being the membership value of R in the fuzzy set f. Evidently, g_P^f is a fuzzy disk with $g_P^f(P) = f(P)$ and $g_P^f \leq f$ (i.e., g_P^f is a subset of f). Moreover, it is easy to see that

$$\sup_{P \in D} g_P^f = f.$$

Let C be any subset of D such that for all $P \in D$, there exists $Q \in C$ for which $g_P^f \leq g_Q^f$. We call such a set C an f-sufficient subset of D. Evidently, for any such subset C we have

$$\sup_{P \in C} g_P^f = f. \tag{4}$$

In other words, the set $\{g_P^f \mid P \in C\}$ can determine f. If D is finite, and we make C as small as possible, $\{g_P^f \mid P \in C\}$ is a compact representation of f.

In particular, let D be a digital image X and f be a fuzzy representation of X, i.e.,

$$X = \{f(P) \mid f(P) \in [0, 1]\}.$$

For example, $f(P)$, the normalized gray value of a pixel P may be viewed as a degree of its belonging to f (or the degree to which the pixel P is bright, say). We say that $P \in D$ is a (nonstrict) local maximum of f if P has no neighbor Q such that $g_P^f < g_Q^f$. Let C_f be the set of such (nonstrict) local maxima of f. Evidently, the set C_f is an f-sufficient subset of D, so that f is the sup of the g_P^f's for all $P \in C_f$. In other words, the pixel intensity $f(t)$ at a point t of the image can be obtained from

$$f(t) = \max_{P \in C_f} g_P^f(t), \tag{5}$$

because t has its maximum membership value $(=f(t))$ to one of the disks g_P^f, $P \in C_f$. The set C_f is called the *Fuzzy Medial Axis* (FMA) of f, and $\{g_P^f \mid P \in C_f\}$ is called the *Fuzzy Medial Axis Transformation* (FMAT) of f. If f is a crisp subset of D i.e., $f \in \{0, 1\}$, the aforesaid definitions reduce to the standard definitions of the MAT (as described in Section 2).

The definition of the FMAT is thus seen to involve natural extensions (generalization) of the concepts of maximal disk, union, inclusion and symmetry for an ordinary set to a fuzzy set. For a gray tone image X (the gray values being normalized in the range $[0, 1]$), it computes, first of all, the various fuzzy disks centered at the pixels and then retains a few (as small as possible) of them, as designated by g_Q's, so that their union can represent the entire image X.

3.1. Example

Consider a 5×5-image X as shown in Figure 5. The lower left pixel of intensity 4 has coordinate $(1, 1)$. Fuzzy disks are computed with d_8-metric. The center pixel has $g_P = \{7, 6, 4\}$.

5	5	5	5	5
5	6	6	6	5
5	6	7	6	5
5	6	6	6	5
4	5	5	5	5

Fig. 5. 5×5 digital image. Pixels belonging to fuzzy medial axis (FMA) are marked bold. Pixels belonging to reduced fuzzy medial axis (RFMA) are underlined.

(Note that the gray values are not normalized in $[0, 1]$. Pixels outside the image are assumed to be of zero intensity while computing the disk values. The superscript f is omitted.) Here, the first entry denotes the non-normalized membership value of the pixel itself to the disk $g_{(3,3)}$, i.e., g_P-value at zero distance or at radius $r = 0$. The second and third entries denote, respectively, the membership values of the pixels, which are at distances 1 and 2 from the center pixel, for the disk $g_{(3,3)}$. For the pixels having intensity 6, g_P has the pair of values $\{6, 5\}$ except the one at $(2, 2)$ which has $\{6, 4\}$. These entries correspond to $r = 0$ and 1; the g_P-value at $r = 2$ is zero. For the pixels on the border of the image, g_P is specified by the single value $f(P)$. The g_P-values are zero for $r = 1$ and 2.

The pixels constituting the fuzzy medial axis C_f are marked bold in Figure 5. The disks g_P around these pixels define the fuzzy medial axis transformation of the image X. Note that for any pixel $P \in X$, there exists a pixel $Q \in C_f$ which satisfies the (subset) criterion $g_P(t) \leq g_Q(t)$ for all points t in the image. Since the g_P of the center pixel is defined by a triple of values, there is no other pixel for which the above subset condition can be satisfied; so it is treated as a member of C_f. Similarly, for the g_P's of all the pixels having value 6, except the one at $(2, 2)$, the subset condition is not satisfied when the center pixel is considered as Q. For example, consider the pixel at location $(2, 4)$ as P. Let the pixel at location $(1, 5)$ be considered as t. Then the values of $g_{(2,4)}(t)$ and $g_{(3,3)}(t)$ denoting the membership values of t corresponding to the fuzzy disks centered at the points $(2, 4)$ and $(3, 3)$ are 5 and 4, respectively. Therefore, the criterion $g_{(2,4)}(t) \leq g_{(3,3)}(t)$ for all $t \in X$ is not satisfied. For the border pixels of intensity 5, the subset condition is satisfied by one of the 6's in C_f, whereas it is the center pixel which makes the condition satisfied for the lower-left pixel 4.

In order to reconstruct the input image, i.e., to restore the deleted pixels, simply put all the disk values of FMA pixels at those locations back. In case a location has more than one such value, select the largest one. For example, if we want to get the intensity back at the point $(2, 2)$, then put all the disk values (which are 6, 5, 5, 0, 0, 0, 0, 0) of the eight FMA pixels at that point. Since there are eight values, select the largest

one, i.e., 6 as the intensity at the point (2, 2). Similarly, to get the intensity back at the location (1, 1), take the largest among $\{4, 0, 0, 0, 0, 0, 0, 0\}$.

3.2. Some remarks

(i) The number of the FMA pixels in X, denoted by $|C_f|$ or |FMA|, is dependent on both r, the radius (or extent) of fuzzy disk used and the crispness of X. With increase of the crispness (contrast between object and background, say) in X, $|C_f|$ tends to decrease. Its minimum value corresponds to the two tone version of X. As r decreases, $|C_f|$ increases because the possibility of a disk g_P being maximal increases. In other words, the likeliness of the condition $g_P \leq g_Q$, $P \neq Q$, being satisfied for any P decreases with decrease in r. (In the limiting case when $r = 0$, FMA of an $(M \times N)$-dimensional image is the image itself and $|C_f| = MN$.) These were explained in [9].

Again, the increase in r after a certain value, say r', may not cause further reduction in $|C_f|$ by making some more pixels P satisfy the subset property $g_P \leq g_Q$. The higher the fuzziness in X, the greater will be the value of r'.

(ii) It is seen from Figure 5 that specifying the FMAT requires 17 values (1 disk requires 3 values, 7 require 2 each), as compared to 25 values required by X itself. For real images, the situation becomes even worse [9]. (Note that if we had the pixel intensity 4 of X replaced by 5, the FMAT would have been reduced to only one disk with $g_{(3,3)} = \{7, 6, 5\}$.)

(iii) It is found to be computationally very expensive if one needs to check the inclusion (subset) condition of a fuzzy disk $g^f_P(t)$ by another disk $g^f_Q(t)$ for all P, Q and t in the image f.

In the following sections, we will be explaining some concepts and algorithms developed on these issues, namely, reducing redundancy in FMAT, extracting various approximated versions of FMAT and the related computational aspects in order to make these tasks efficient, so that the FMAT can be made practically feasible.

4. Redundancy removal (RFMAT)

The removal of redundancy in pixels (fuzzy disks) from the fuzzy medial axis output is made by considering the criterion

$$g^f_P(t) \leq \sup g^f_{Q_i}(t), \quad i = 1, 2, \ldots \tag{6}$$

instead of

$$g^f_P(t) \leq g^f_Q(t). \tag{7}$$

For example, the representation of the FMAT in Figure 5 is seen to be redundant. Note that the point at location (3, 4) can be removed because it is contained in the union of the fuzzy disks around (3, 3) and (2, 4) (or (4, 4)), i.e.,

$$g_{(3,4)} \leq g_{(3,3)} \cup g_{(2,4)} \quad (\text{or} \leq g_{(3,3)} \cup g_{(4,4)}), \tag{8}$$

or,

$$g_{(3,4)} \leq \max\{g_{(3,3)}, g_{(2,4)}\} \quad (\text{or} \leq \max\{g_{(3,3)}, g_{(4,4)}\}), \tag{9}$$

for all pixels in X. Similar is the case with the pixel at location (4, 3) which can also be removed. The pixels representing the final reduced FMA are underlined in Figure 5. Let RFMAT denote the FMAT after reducing its redundancy.

It therefore appears that one needs to go through a lengthy searching procedure to determine for every pixel P, a set of Q's (local maxima) which can satisfy criterion (6) of containment in order to delete P. An efficient way of performing this task is explained below.

The algorithm checks in a preferential sequence (from exterior to interior) with every pixel, how many pixels it is sponsoring (representing) and whether the current pixel along with the ones it is sponsoring can all be replaced by some other (or a combination of others). A pixel P is said to be sponsored (or represented) by a pixel Q at a distance r if its normalized intensity $f(P)$ equals $g_Q(P)$, the membership value of P to the fuzzy set around Q. Obviously, P can have more than one sponsoring pixel other than itself. In such a case, P can be deleted because $f(P)$ can be reconstructed from its sponsoring pixels, i.e.,

$$f(P) = \sup_{k \in N} g_k(P), \tag{10}$$

N being the set of neighboring pixels of P at a distance r.

Now, satisfying criterion (6) means that the fuzzy disk g_P is a subset of the union or combination of some other disks $g_{Q1}, g_{Q2}, \ldots$, and therefore the pixel P and the ones it is

sponsoring (representing) can all be sponsored by a set of pixels $Q1$, $Q2$, ... In such a case, P can be deleted, i.e., not treated as a member of the MA because $Q1$, $Q2$, ... can take care (in the sense of representation) of both P and its sponsoring pixels.

By the rank of a pixel P we mean the extent to which the values of $g_P(r)$, $r = 1, 2, \ldots$, are nonzero. The higher the rank of a pixel (or disk), the greater is its possibility of being treated as a maximal fuzzy disk or a strong sponsor (i.e., as a number of MA). The aforesaid ranking system provides a spatial preference among the disks (or pixels) in order to facilitate the process of considering a pixel for its possible deletion. That is why the algorithm checks from exterior to interior with every pixel for its possible deletion. This also enables one to provide a compact representation of the (object) region of our interest, which may be assumed to be in the interior part of the image.

4.1. Algorithm

The aforesaid concept of deletion of pixels is further explained in Figure 6 for the convenience of writing a computer program. The arrows from a few border pixels point to their respective sponsors. (In case a pixel gets more than one sponsor, we select the one which comes at left-most (for horizontal) or uppermost (for vertical) position.) The central point is seen to sponsor all the pixels having intensity 6 at $r = 1$, plus the pixel (which has intensity 4) at $r = 2$.

Let us now consider the circled pixel for its possible deletion. This pixel is sponsoring only the triangled pixel. It is further seen that the triangled pixel can also be sponsored by the squared pixel (denoted by the dotted arrow) which is currently sponsoring three pixels, and the circled pixel itself can be replaced by the center pixel having highest intensity. Therefore, the circled pixel can be deleted from the MAT representation because, this pixel and the pixel it was sponsoring can now be covered by the center pixel and the squared pixel together; thereby making them more responsible (i.e., stronger sponsor). Successive deletion of the pixels, in this way, from exterior to interior will ultimately result in the reduced FMAT (RFMAT).

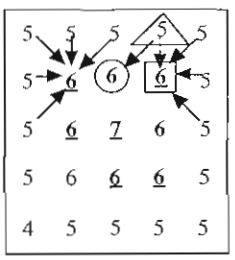

Fig. 6. Sponsoring and deletion procedure.

Although the technique for reducing redundancy has been developed here for a gray tone image, it is well applicable for a binary image, too. It is further to be noted that, for checking of criterion (6) for a particular pixel P, one need not search over the entire image space for determining a set of Q's. Similar is the case with checking criterion (7) for all Q and t. In the following section, we will explain how the time of computation of FMAT can be reduced significantly by restricting the searching space.

5. Reducing the searching space

Let n_P and n_Q be the number of membership values of the fuzzy disks centered at P and Q, respectively. Let $d(P, Q)$ denote the distance (d_8-metric of (2)) between P and Q. A careful investigation of the definition of FMAT then reveals the following criteria for checking with every pixel P the condition $g^f_P(t) \leq g^f_Q(t)$:

$$n_P < n_Q, \tag{11a}$$

$$d(P, Q) < n_Q, \tag{11b}$$

$$t \in S_P, \tag{11c}$$

where S_P denotes the supporting points of P, i.e., the points for which $g^f_P(t) > 0$. The underlying concept is that the set of supporting points of the upright square fuzzy disk (since we are using d_8-metric) centered at Q should include those of P, i.e., $S_P \subset S_Q$. These conditions allow working with a much smaller subset of an image and therefore reducing the time of computation.

Similarly, for determining a sponsor Q for a given P, while reducing the redundancy in FMAT, the criterion followed is simply

$$d(P, Q) \leq n_Q. \tag{12}$$

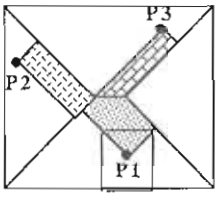

Fig. 7a. Searching space of Q and t for computing FMAT.

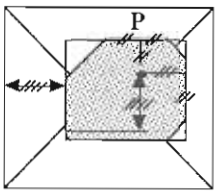

Fig. 7b. Searching space of Q for computing RFMAT.

It is to be noted from Figure 6 that the consideration of t's does not arise here.

The significant reduction of searching space while computing the FMAT of an image and reducing its redundancy is explained graphically in Figures 7(a) and 7(b), respectively. The shaded portions represent the domain of Q to be only considered for a particular P. The square at the bottom of Figure 7(a) indicates the domain of t corresponding to $P1$.

Note that the number of rows M and number of columns N considered here are different. There are four bisectors drawn from four corners of the image. They meet at the center and split the image space into two triangles and two trapezoids. (The splitting may result in four triangles or four trapezoids depending on the values of M and N.) For a given P in Figure 7(a), two lines are then drawn at an angle of ± 45 degrees with the horizon. The space covered by these lines with the two closest bisectors constitutes the domain of Q. Similarly, the square drawn with length equal to twice the distance of P from its nearest boundary constitutes its domain of t.

In the case of Figure 7(b), first of all, draw two horizontal and two vertical lines placed at half the distances of P from the boundaries. The rectangle thus formed by their intersections constitutes the maximum possible domain of Q. This rectangular region is further reduced by truncating the corners according to criterion (12). These graphical representations are given for the convenience of writing an efficient program.

6. Methods of approximation (AFMAT)

The RFMA output of an image X as obtained in the previous section can be regarded as a generalized fuzzy axis of symmetry and provides a kind of skeleton (of the elongated regions) of X by allowing it to be a fuzzy subset of the image. The set of disks $\{g_P \mid P \in \text{RFMA}\}$ provides a compact representation of the fuzzy set f characterizing the image X. The value of $f(P)$, $P \in \text{RFMA}$, may be viewed as denoting the degree of belonging of P to the fuzzy subset 'medial axis' of X as far as its compact representation (and hence exact reconstruction) is concerned.

Since specifying the FMAT, even after reducing redundancy, needs more storage, we will be describing here three different types of procedures for approximating RFMAT and/or reconstructed output (for more economical representation without affecting the reconstruction much) of an image.

6.1. *Approximation during reconstruction* (Method 1)

The approximation technique described here has the following two steps:

Step 1. Construct RFMAT of an image X using fuzzy disks of radius r, say.

Step 2. Reconstruct the image with disk values from 0 to z, $z < r$.

This means that the storage space of X is reduced simply by keeping a few lower radii (truncated) disk values for the purpose of its reconstruction. The extent of the exactness of reconstruction is obviously dependent on the value of z. The smaller the value of z, the lesser is the storage requirement and the lower will be the exactness in reconstruction. (Note that $z = 0$ corresponds to the RFMA output.)

6.2. *Approximating* RFMAT (Method 2)

The previous algorithm does not involve any approximation on the RFMAT output; it only truncates the disk values during reconstruction. That is, the number of disks remains the same.

0	0	0	0	0
0	6	0	5	0
0	2	5	0	0
0	0	3	4	0
0	0	0	0	0

Fig. 8. Sponsoring capability map of RFMAT in Figure 5.

The present algorithm, on the other hand, makes an approximation on the FMAT itself by truncating off a set of disks, while keeping the radius of disks unchanged. The truncation is achieved based on the importance of an individual RMA pixel (or RMA fuzzy disk) on the basis of its sponsoring capability. The higher the sponsoring capability of a pixel (or disk), the more is its importance in representing the image.

Let us consider, for example, the sponsoring capability map (Figure 8) of the RFMA output of Figure 5. Here, the set of 0's means that the corresponding pixels are deleted because these have been taken care of by others. The number '1' implies that the corresponding MA pixel sponsors only itself. '2' corresponds to a pixel which can sponsor one other than itself, and so on for other numbers in Figure 8. The histogram of Figure 8 will therefore represent the number of MA pixels with different sponsoring capabilities, e.g., it has 19, 0, 1, 1, 1, 2, 1 pixels with capability 0, 1, 2, . . . , 6, respectively. (The sum of these values is equal to the total number of pixels in X.) For real images, the histogram is usually seen to have monotonic non-increasing behavior. This leads one to eliminate a large number of low-sponsoring pixels from the MA, thereby making the image representation economical without affecting much of its reconstruction. For example, if we delete the MA pixel at location (3, 2) of sponsoring capability 2, it will produce an approximated reconstruction with the original pixel value 5 at the point (2, 1) being changed to 4.

The algorithm therefore has the following three steps:

Step 1. Construct RFMAT of an image X using fuzzy disks of radius r, say.

Step 2. Construct sponsoring capability map of RFMAT output (i.e., of RMA pixels).

Step 3. Select a sponsoring capability number T, say, and delete all the MA pixels of sponsoring capability $\leq T$.

The degree of exactness in reconstruction will obviously depend on the number of deleted MA pixels and their sponsoring capability. The higher these values are, the lower is the exactness. It will also depend, to some extent, on the value of r. These will be demonstrated in Section 7.

6.3. *Extracting an optimum compact* RFMAT (Method 3)

The techniques described in the previous two algorithms affect the pixel intensities over the entire image by making the approximation distributed. In many applications, we are more interested (or only interested) in the MA of the object regions represented by darker pixels. In that case one may delete from the RFMA output some of the pixels (or disks) representing the medial axis of background (i.e., lighter) regions; thereby resulting in an approximate medial axis of X.

A technique is described here to perform this task automatically, where the deletion process is guided by the principle of minimizing ambiguity in the geometry (or in the spatial domain) of RFMA. In other words, considering a fuzzy subset μ defined over the FMA output of X, its optimum (in the sense of minimizing ambiguity in geometry) version can be extracted from one of its α-cuts having maximum 'compactness' value. This optimum version may be viewed as an approximate MAT representation of the image X, because it keeps only a set of darker MA pixels (to an optimum amount in the sense of maximizing compactness) for representing the object regions of our interest and ignores the rest.

The extent of reconstruction, particularly the background region, will be determined by the radius r of the remaining disks. The larger the disk radius, the more will be the coverage of background region. Before describing the method of obtaining an optimum FMAT, let us give the definition of compactness of a fuzzy set.

Compactness of a fuzzy set

Let μ denote a piecewise constant fuzzy representation of an image X. Compactness of μ

is defined as [3–5, 11]

$$\text{Comp}(\mu) = a(\mu)/p^2(\mu), \tag{13}$$

where

$$a(\mu) = \sum_i \mu_i \tag{14}$$

and

$$p(\mu) = \sum_i \sum_j \sum_k |\mu_i - \mu_j|\,|A_{i,j,k}|,$$
$$i, j = 1, 2, \ldots, r,\ i < j,\ k = 1, 2, \ldots, r_{ij}, \tag{15}$$

denote the area and the perimeter of μ, respectively. $a(\mu)$ is the weighted sum of the area of the regions on which μ has constant value, weighted by these values. $p(\mu)$ is the weighted sum of the length of the arcs $|A_{ijk}|$ along which the i-th and j-th regions having constant values μ_i and μ_j, respectively, meet, weighted by the absolute difference of these values.

Optimum α-cut

Let μ denote the fuzzy set representation of RFMA output of an image X. Let each element of this output be normalized so that its membership value $\mu(P)$ can lie in $[0, 1]$. The α-cut of such a μ-plane is defined as

$$\mu_\alpha = \{P \in \text{RFMA} \mid \mu(P) \geq \alpha\}, \quad 1 > \alpha > 0. \tag{16}$$

Modification of α will therefore result in different approximated FMA planes with varying Comp(μ)-value. As α increases, the Comp(μ)-value initially increases to a certain maximum (peak) and then for a further increase in α, the Comp(μ)-measure decreases.

The initial increase in Comp(μ)-value can be explained by observing that for every value of α, the background medial axis pixels having μ-value less than α are not taken into consideration. So both area (see (14)) and perimeter (see (15)) are less than those for the previous value of α. But the decrease in perimeter is more (since the lighter pixels representing the MA of the background are highly disconnected, they have high perimeter value) than the decrease in its area and hence the compactness (cf. (13)) increases (initially) to a certain maximum corresponding to a value $\alpha = \alpha'$, say.

Further increase in α (i.e., for $\alpha > \alpha'$), results in a μ_α-plane consisting mainly of the object (darker) MA pixels which are not much disconnected (because most of the lighter or background MA pixels which were highly disconnected have already been dropped out). As a result, the decrease in area here is more than the decrease in perimeter, and Comp(μ) decreases. The μ_α-plane having a maximum compactness value can be taken as an optimum (in the sense of compact representation of μ) FMA (and hence FMAT) for the (object) regions of our interest in the image X. This optimum version may also be treated as an approximate FMAT representation of the image X, because it retains only an optimal (in the sense of maximizing compactness) set of darker MA pixels for representing the object region and ignores the rest.

Note further that the $\mu_{\alpha'}$-plane, as obtained above, can be regarded as a subset denoting the optimum fuzzy skeleton of elongated regions of the image X. The plane $\mu_{\alpha'}$ is most compact and has minimum spatial ambiguity as far as its skeleton extraction is concerned.

7. Experimental results

Figure 9 shows a 36×60, 32-level input image of 'S'. Figure 10(a) is its FMAT output, after reducing redundancy in the medial axis, when the fuzzy disks are computed only up to the radius $r = 2$ (i.e., disk values at radii 0, 1 and 2 are only considered for computing the FMAT). The number of resulting disks in Figure 10(a) is 943. This consists of 781 disks with 3 membership values and 81 disks each with 2 and 1 membership values; thereby making the total number of values equal to 2586. (Note that specifying the original image (Figure 9) itself needs only 2160 ($= 36 \times 60$) values.) The situation becomes even worse for larger values of r which leads to having less disks but with a larger number of total membership values for its exact representation. This is illustrated in Table 1. For example, the RFMAT output corresponding to $r = 9$ needs 879 disks with total number of values equal to 5449 (271 disks, 45 disks, 48 disks, 58 disks, 61 disks, 80 disks, 73 disks, 81 disks, 81 disks and 81 disks with

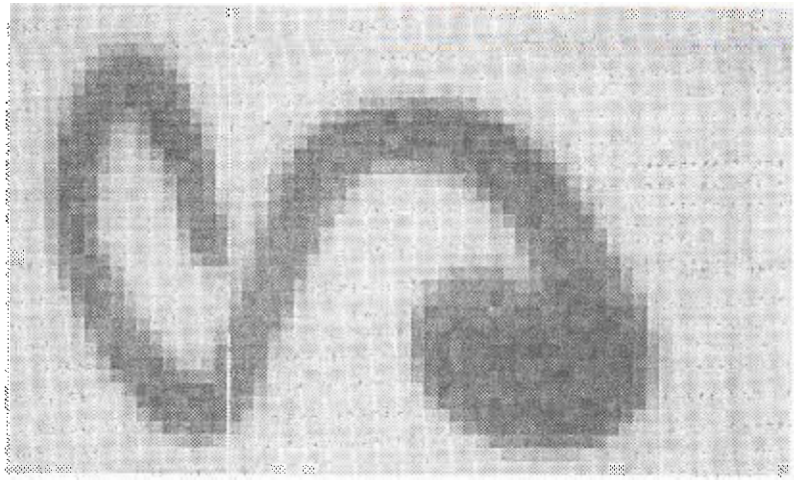

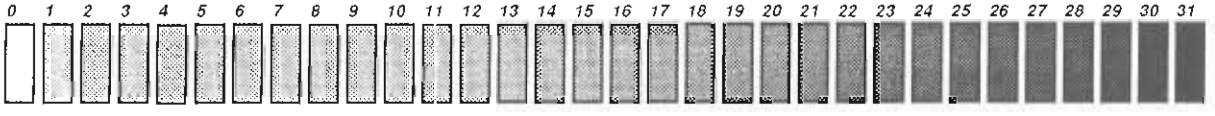

Fig. 9. 36×60 'S' input image.

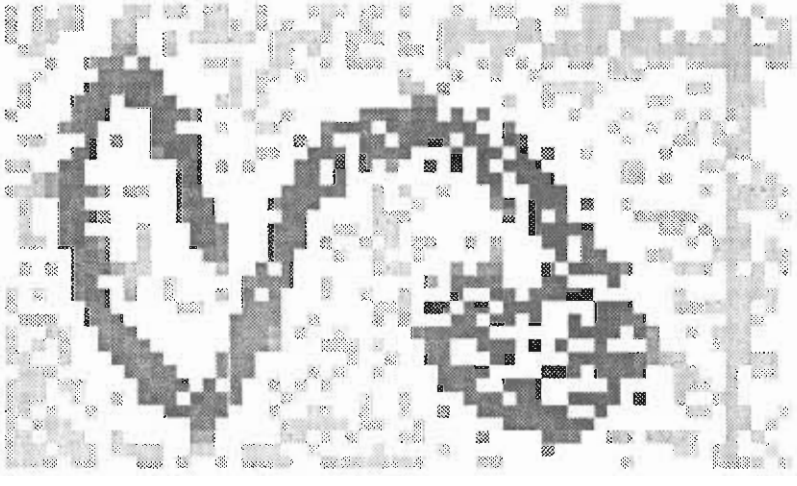

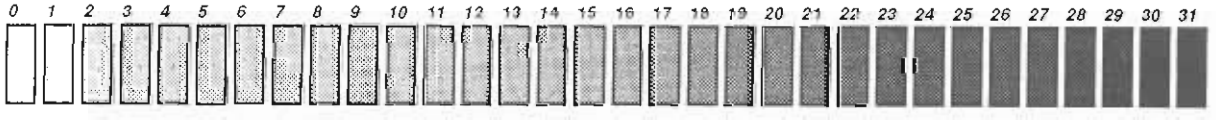

Fig. 10a. RFMAT output of Figure 9 for $r = 2$.

membership values $10, 9, 8, \ldots, 1$, respectively). If we increase the disk radius to 17 (maximum value), the image still needs 879 disks, but the aforesaid 271 disks, each of 10 membership values, have now been split up into 44, 40, 36, 36, 28, 27, 26, 18, 16 disks with membership values $10, 11, 12, \ldots, 18$, respectively. As a result, the total number of membership values to specify the image increases to 6326. The corresponding RFMAT

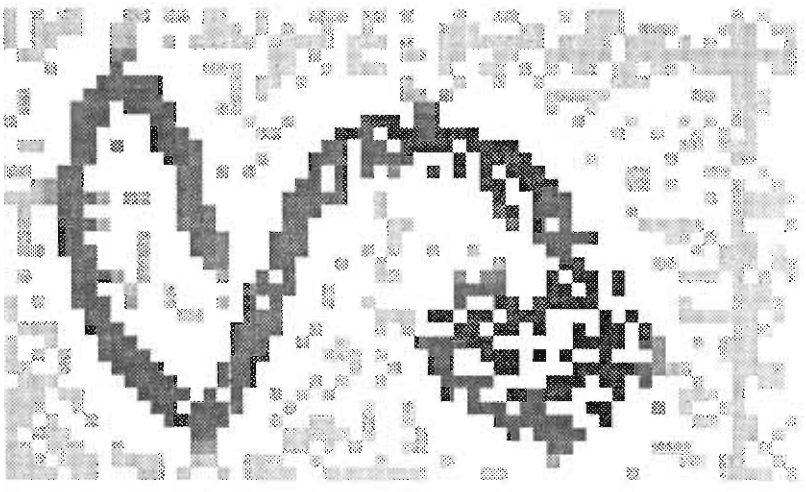

Fig. 10b. RFMAT output of Figure 9 for $r = 17$.

Table 1. Variation of number of fuzzy disks and membership values with radius r for computing RFMAT of 'S' image

Radius	Fuzzy disks	Membership values
17	879	6326
15	879	6276
14	879	6216
10	879	5676
9	879	5449
8	880	5187
6	883	4526
5	885	4112
4	890	3648
3	901	3118
2	943	2586
1	1126	2165
0	2160	2160

output is shown in Figure 10(b). (For $r = 0$, the RFMAT is just the entire set of pixels in the image.)

Figures 11 and 12 show the sponsoring capability map (number of pixels being sponsored by an individual MA pixel) and the sponsoring capability histogram (number of occurrences of the MA pixels of different sponsoring capabilities) of the RFMAT output in Figure 10(a). As expected, Figure 12 has a monotonic non-increasing behavior.

Figure 13 shows the reconstructed output using Method 1 for three possible combinations of r and $r1$. Comparing Figure 13(a) with Figure 13(b), it is seen that Figure 13(a) has less pixels missing (blank) because it has been prodnced with a comparatively larger number of disks. Furthermore, most of the uncovered pixels are seen to lie around the edge of the object region. This is obvious from their RFMAT output (Figure 10) which shows that the corresponding pixels were taken care of by other, particularly by object pixels at distance $d_8 \geq 2$. Since all the disks after radius $r \geq 2$ have been truncated, those lost pixels could never be recovered. Even keeping one more radius (i.e., truncating disks after $r \geq 3$) could not avoid entirely the appearance of these blanks (see Figure 13(c)). The total number of membership values cut down by this approximation method is explained in Table 2.

Figure 14 shows the reconstructed output using Method 2 for four possible combinations of r and T. Figure 14(a) corresponds to the case when all the 329 MA pixels of sponsoring capability 1 (Figure 12) have been deleted. The image (Figure 14(a)) thus reconstructed from the

```
1 1 11   11 11 11  1   111 11 1   1  11   1 111        1 1
1 3112  31     223 4 3  2  2     322   42   223 333   242 31
1 51    23  4 23231 25221 143 5  42421115 3112 212 4 2 11  1
 24     32  7       13 2  5   32 22  11  72221 2111151111321
   2  733 4    321  15  1 228    1  12 1 1 12 11 61 21122 41
  4    11222     1 21 1       1   4  1  2     511      22
 1    222213     2 1          22 2       31211      42 216
 1   323 1143   21 4            21     3  1  1    31    315
1    323   2243   2  1     334323 3 4      2   5   2 1 13
    533    32   2  11   5233 2113231  5       9  1  1 2 3
 62   3 2  2232       3 2  32 1322 26 23       4   11 122
     63    2422    12  137 3211   3 42 3 5  3     1    31
13  24       33 6 2   33 3 2 2  3 2 3 231      14    73  2
  1242       33       22 3          33 333     62 2    1 51
11112231 41  24      23333  3 3  5   3  233          7 51311
 1  42       314    4332    1  5     23 413 6  4       3111
 4  2226     232     12     131       3 3 4     14222  2   1
 2  31    5   233   243  41 11          23123     22 2 11
 12 3211  3   233   231 6  2 3 11  2 1   25 3       2 312 7
     312  2    23   53   3  4  1     2    1 33   11   312 11
 6 2 312221     3  6 3      411   3 42   1 21326   122 1 2 1
     32  1  4     2233  4       2 3222   11   1        111
1 2  232 1  4   1 3 3   4  4  1   3  32 12118      8   1311
1     23     11   222       211 33 42 211    222   322121 4
 223  233        1221  2    1 3   23 11 2  4 2222      223
1  33  333       5115 4  3     443111       3222 22  1 412
1 1 2  3333      2332   123 6   32  833 B 1  1   3    111
12  2   3333    322       2  2  33   21    623213311   1511
 121     3232   333    2 4  2    3112    311 1323  21  1 24
112 11    3132 2 3  3 2 1         231  221     3    215 6
112  6  4 333 3233   1     9  3    331 11  3143 5  3  52
11 2  2     34233   4  12  1  2  5  3321111  2      21 14  1
1 211          43     22212 44  1      3342133          21 2
11 211  1      32     21 4 3   22    6    833  45 3213  2 2
111 111 5133  11  211  1    1    3       1         11 13  4
1111 11   11 1  1 1111  11111111    11          1      1111 1
```

Fig. 11. Sponsoring capability map of Figure 10a. The alphabets A and B correspond to the numbers 10 and 11.

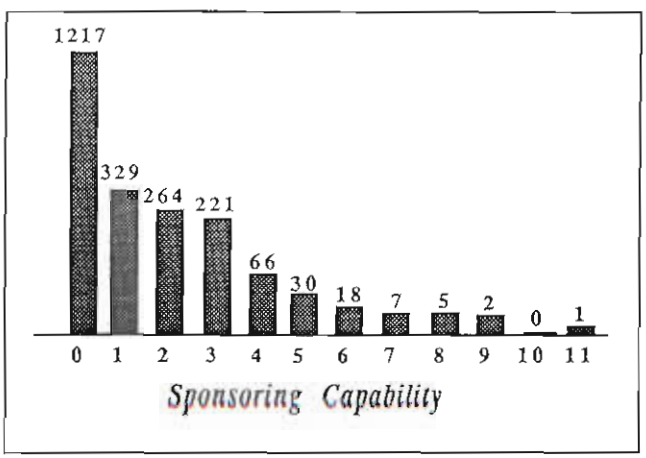

Fig. 12. Sponsoring capability histogram of Figure 10a.

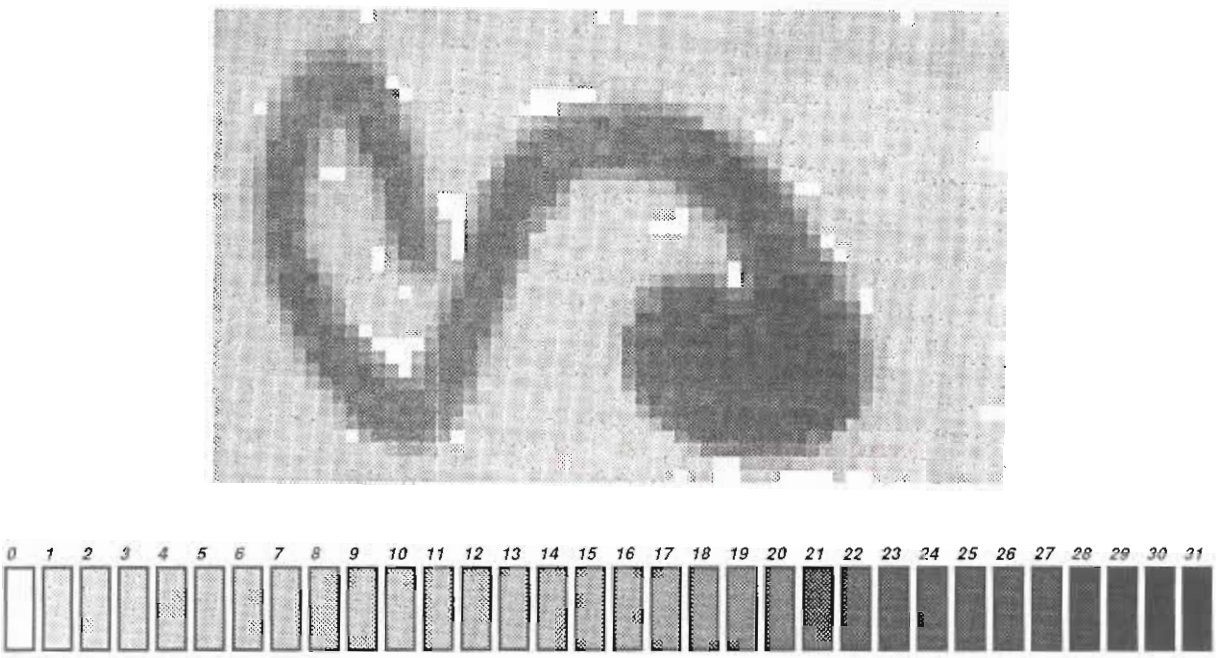

Fig. 13a. Reconstructed output using Method 1, with $r = 2$ and $z = 1$.

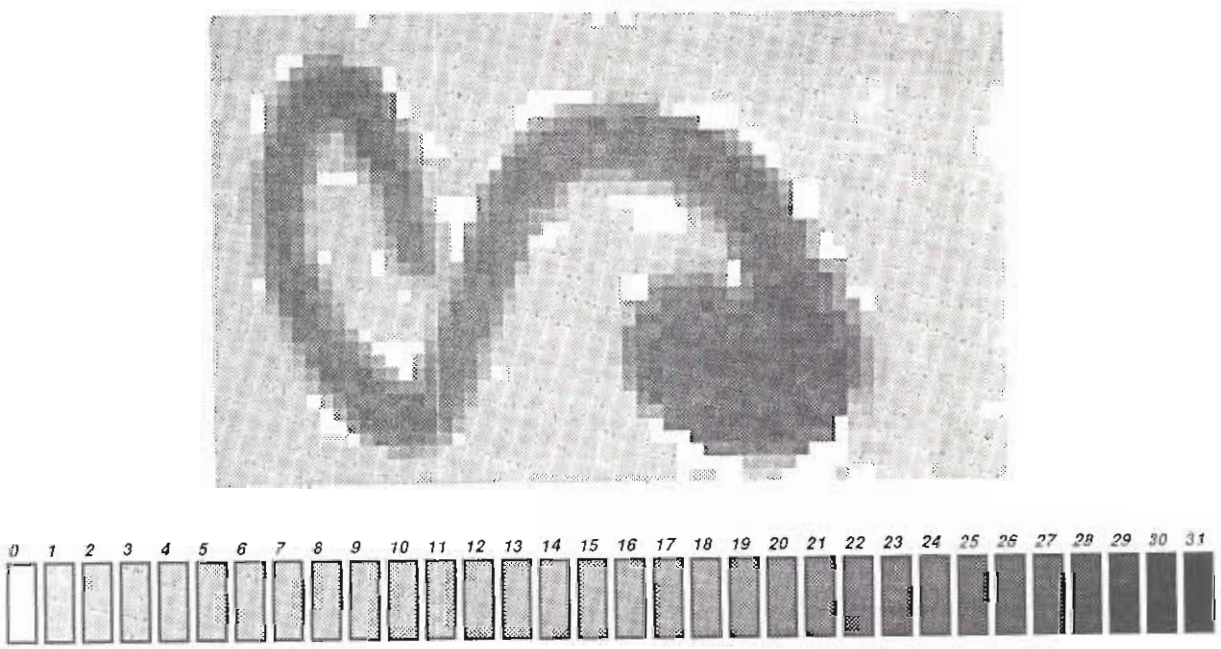

Fig. 13b. Reconstructed output using Method 1, with $r = 17$ and $z = 1$.

truncated RFMAT still looks very similar to the original input. Note that the number of fuzzy disks remaining after truncation is 614. This consists of 568 disks with 3 membership values and 46 disks with 2 membership values, thereby making the total number of values in the truncated FMAT equal to 1796. Figure 14(b) shows another approximated output when all the 264 MA pixels with sponsoring capability 2 are further deleted. This brings the total number of

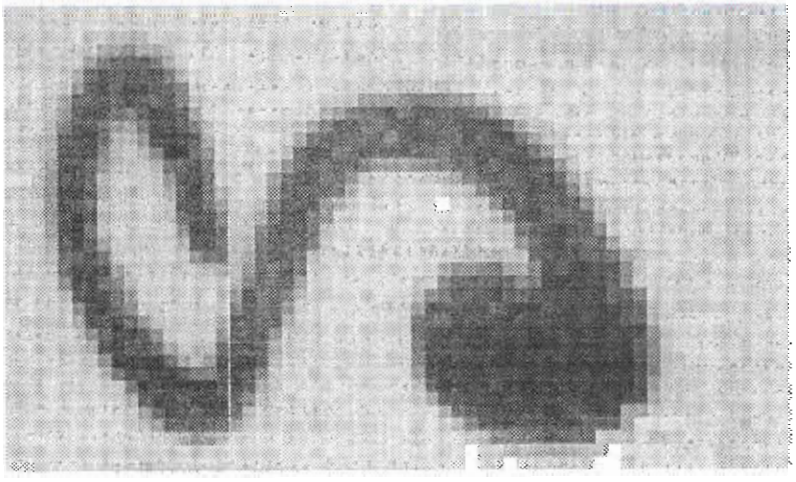

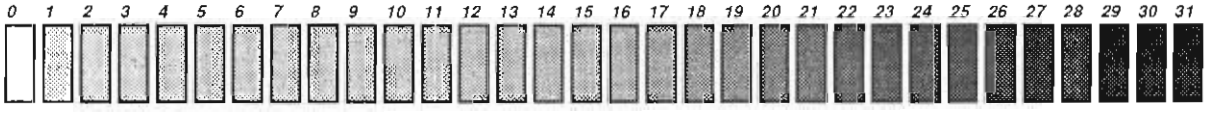

Fig. 13c. Reconstructed output using Method 1, with $r = 17$ and $z = 2$.

Table 2. Number of fuzzy disks and membership values for different approximated FMAT (AFMAT) versions of 'S' image

AFMAT	Fuzzy disks	Membership values
Fig. 9a	943	1805
Fig. 9b	879	1677
Fig. 9c	879	2394
Fig. 10a	614	1796
Fig. 10b	350	1023
Fig. 10c	512	4384
Fig. 10d	345	3136
Fig. 11a	368	1095
Fig. 11b	343	3567

membership values in the truncated FMAT further down to 1023 (323 fuzzy disks with 3 membership values and 27 disks with 2 membership values).

The approximated RFMAT (AFMAT) versions corresponding to $r = 17$ (Figures 14(c) and 14(d)) have number of disks equal to 512 and 345 (Table 2). Since these disks use maximum possible radius, the approximated representation of FMAT does not turn out to be economical.

Table 3 shows the variation of Comp(μ) with α (Method 3) when Figures 10(a) and 10(b) are respectively, considered, as input. The maximum (peak) values are asterisked. The optimum RFMA versions corresponding to the global maximum Comp(μ)-values are shown in Figure 15 along with the reconstructed images (Figure 16) obtained from them.

The reconstructed images demonstrate the capability of the algorithm in providing automatically an optimum FMA which provides a good skeleton, and is very effective and economical (in the sense of storage requirement) in representing the object regions. Here again, the use of the maximum possible disk radii (Figure 16(b)) makes the image representation expensive.

8. Discussiou

This paper described some algorithms for reducing redundancy in the FMAT [9], for generating its approximate versions and for reducing the searching spaces for its computation. The ultimate aim is to be able to make the FMAT practically feasible and useful to a gray image for its skeleton extraction and compact representation. The skeleton of a plane region represents its structural shape in a reduced form so that it can be used as a feature or core line for shape analysis/recognition of the region, for

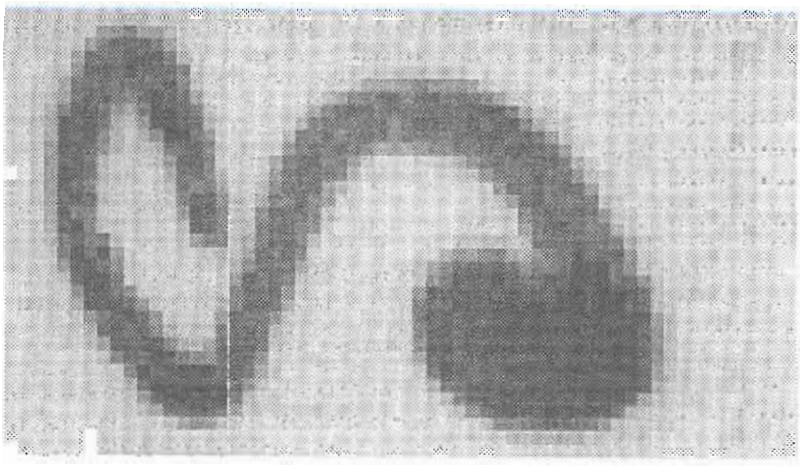

Fig. 14a. Reconstructed output using Method 2, with $r = 2$ and $T = 1$.

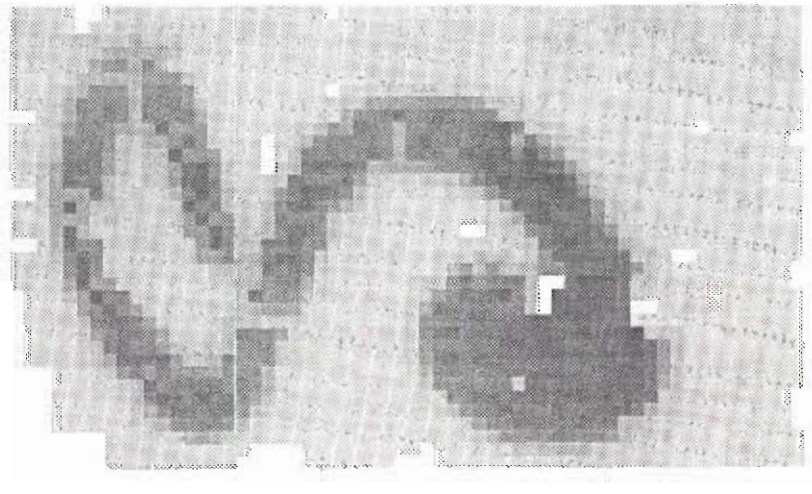

Fig. 14b. Reconstructed output using Method 2, with $r = 2$ and $T = 2$.

representing the image with less storage space and for reconstructing the image.

The computational aspects for the convenience of writing an efficient program have also been addressed. The approximation algorithms initially require the removal of redundancy in the FMAT. Two kinds of approximations are made, namely, the distributed-approximation and the optimum-fuzzy-compactness version. The distributed approximation involves the concept of the sponsoring capability of MA pixels. On the other

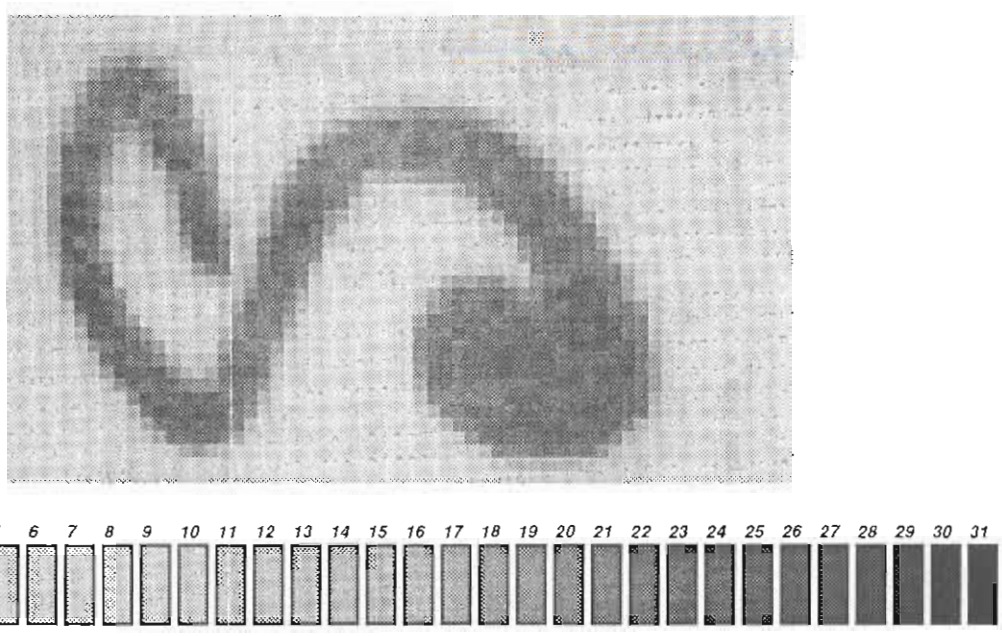

Fig. 14c. Reconstructed output using Method 2, with $r = 17$ and $T = 1$.

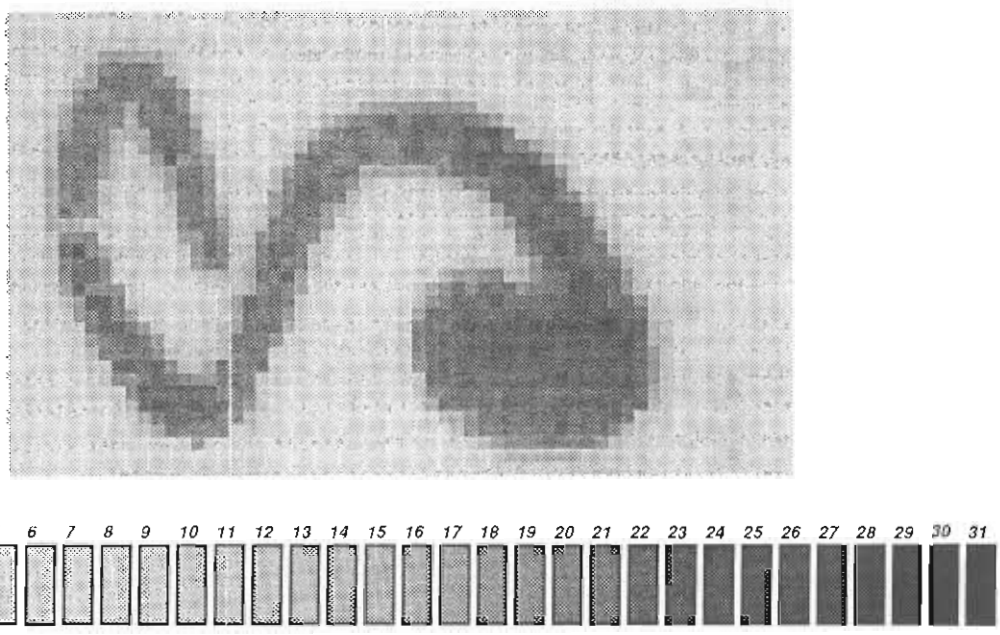

Fig. 14d. Reconstructed output using Method 2, with $r = 17$ and $T = 2$.

hand, the optimum compactness version can be obtained automatically based on the criterion of minimum spatial ambiguity (maximum fuzzy compactness) from the various α-cuts of the fuzzy MA plane.

It is to be noted that for some images, there may not be any optimum (peak) attained in their Comp(μ)-variation with α. In such cases, the α-cut for which there is a 'maximum increase' in Comp(μ)-value of the image may be taken as the optimum one.

The optimum FMA output of the '*S*' image

Table 3. Variation of Comp(μ) with α for Figures 10a and 10b

Non-normalized α	10^4 Comp(μ) Fig. 10a	10^4 Comp(μ) Fig. 10b
0	7.35	7.87
1	7.35	7.87
2	7.35	7.87
3	7.35	7.87
4	7.43	7.95
5	7.62	8.16
6	8.10	8.67
7	9.65	10.34
8	10.56	11.39
9	10.84	11.61
10	11.15	11.93
11	11.24	12.07
12	11.52	12.39
13	11.61	12.43
14	11.94	12.57
15	11.98	12.61
16	12.51	12.82
17	12.61*	12.92*
18	12.55	12.88
19	12.58	12.90
20	12.97*	13.14
21	12.96	13.31*
22	12.43	12.78
23	12.11	11.93
24	12.76	12.85

* denotes maximum.

can be regarded as its optimum fuzzy skeleton (in the sense of minimum ambiguity) where the gray value of a pixel P (i.e., the $g_P(0)$-value), $P \in$ RFMA, denotes the degree of its belonging to the fuzzy subset 'skeleton'. Such skeletons are seen, in a few parts, to be disconnected. The reason (as explained in Section 2.3) is that these are constituted by extracting the maximal fuzzy disks. If a non-fuzzy single-pixel width skeleton is desired, it can be obtained by a contour tracking algorithm [4, 6] which takes into account the direction of the contour, multiple crossing pixels, lost path due to spurious wiggles, etc. based on the octal chain code. Connectivity can further be preserved either by putting back the maximal disks which were initially deleted for reducing the redundancy in the FMAT representation or by inserting pixels having intensity equal to the minimum of those of pairs of neighbors in the object. In such a case, compactness in representation would be further improved.

It would be of interest if some quantitative analysis could be made on the degree of exactness in reconstruction. The measure 'higher-order image entropy' based on the probability of co-occurrence of pixels (and using a logarithmic gain function [7] or an exponential

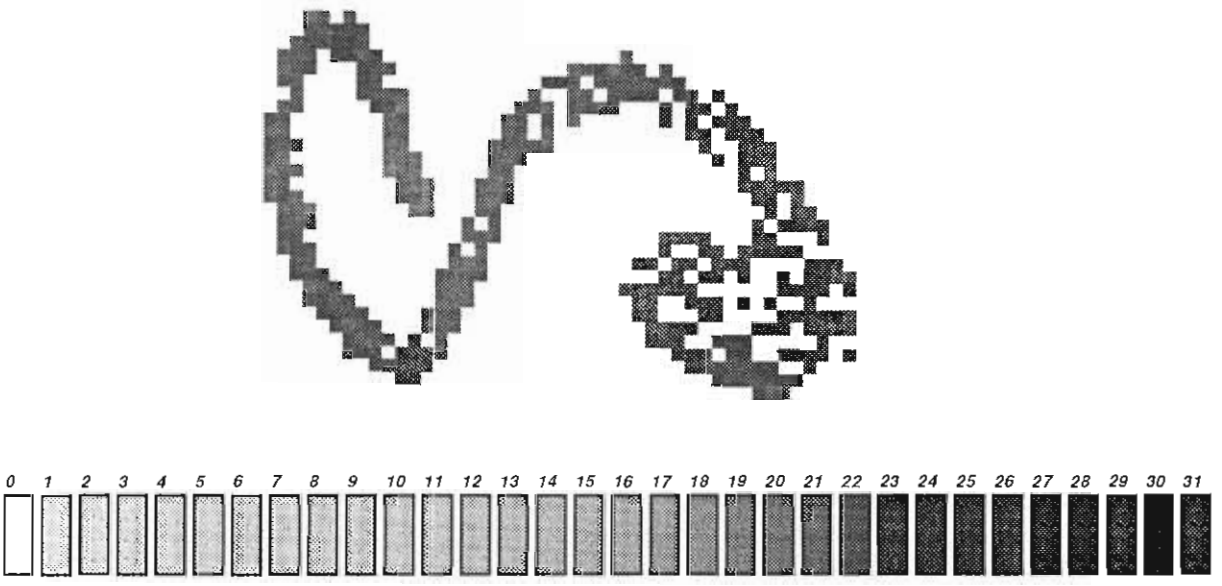

Fig. 15a. Optimum α-cut version of RFMAT output, with $r = 2$ and $\alpha = 20$.

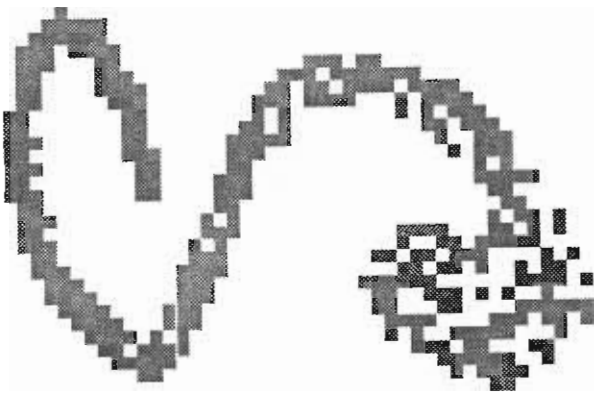

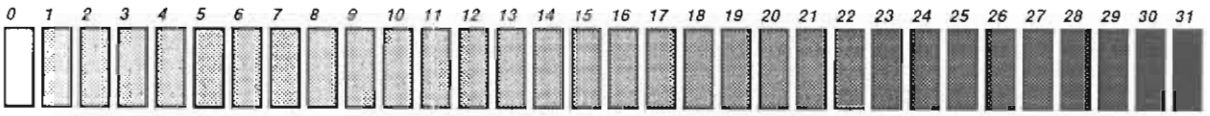

Fig. 15b. Optimum α-cut version of RFMAT output, with $r = 17$ and $\alpha = 21$.

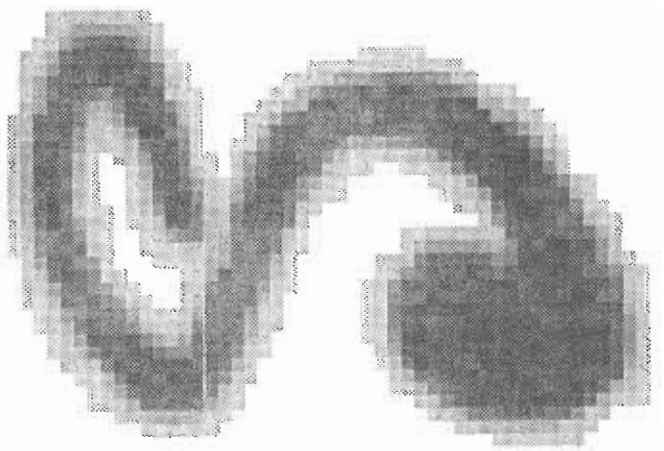

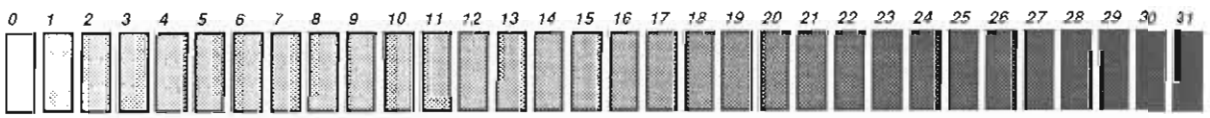

Fig. 16a. Reconstructed output using Method 3, with $r = 2$ and $\alpha = 20$.

gain function [8]) can be used in such an analysis.

The results presented in this paper were computed using d_8-metric (see (2)). If instead of using d_8, we use d_4-distance measure (see (1)), the fuzzy disks will have diamond-like shapes (diagonal square). As a typical illustration, the RFMA output of Figure 5 using d_4-metric is shown in Figure 17. Note that the number of MA disks in Figure 17 is increased, because the uniform regions in Figure 5 are approximated better by the disks of square shape than by those of diamond shape.

Finally, it is to be mentioned here that the

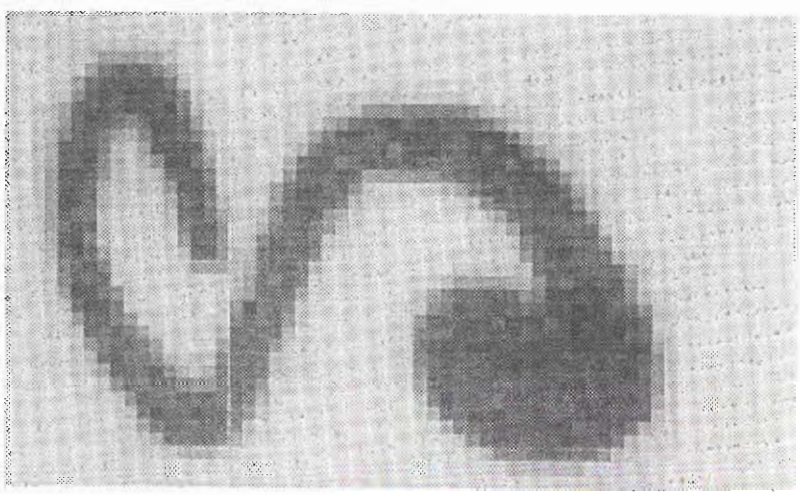

Fig. 16b. Reconstructed output using Method 3, with $r = 17$ and $\alpha = 21$.

```
5           5
  6       6
    7
  6       6
4           5
```

Fig. 17. RFMAT output of Figure 5 using d_4-metric.

algorithms were implemented on a set of various images. To restrict the size of the paper, we have included only the results obtained from one image.

Acknowledgements

This work was done while Dr. S.K. Pal held an NRC-NASA Senior Research Associateship at the Lyndon B. Johnson Space Center, Houston, Texas. He is grateful to Dr. Robert N. Lea for his interest in this work and to the Indian Statistical Institute, Calcutta, for sanctioning him leave from the post of Professor.

References

[1] N. Ahuja, L.S. Davis, D.L. Milgram and A. Rosenfeld, Piecewise approximation of picture using maximal neighborhoods, *IEEE Trans. Comput.* **27** (1978) 375–379.

[2] G. Levi and U. Montanari, A grey-weighted skeleton, *Inform. and Control* **17** (1970) 62–91.

[3] S.K. Pal, Fuzzy skeletonization of an image, *Pattern. Recogn. Lett.* **10** (1989) 17–23.

[4] S.K. Pal and D. Dutta Majumder, *Fuzzy Mathematical Approach to Pattern Recognition* (Wiley, New York, 1986).

[5] S.K. Pal and A. Ghosh, Fuzzy geometry in image analysis, *Fuzzy Sets and Systems* **48** (1992) 23–40.

[6] S.K. Pal, R.A. King and A.A. Hashim, Image description and primitive extraction using fuzzy set, *IEEE Trans. Systems Man Cybernet.* **13** (1983) 94–100.

[7] N.R. Pal and S.K. Pal, Entropic thresholding, *Signal Process.* **16** (1989) 97–108.

[8] N.R. Pal and S.K. Pal, Object-backgrouud segmentation using new definitions of entropy, *IEE Proc. E* **136** (1989) 284–295.

[9] S.K. Pal and A. Rosenfeld, A fuzzy medial axis transformation based on fuzzy disks, *Pattern Recogn. Lett.* **12** (1991) 585–590.

[10] S. Peleg and A. Rosenfeld, A min-max medial axis transformation, *IEEE Trans. Pattern Anal. Mach. Intell.* **3** (1981) 208–210.

[11] A. Rosenfeld, The fuzzy geometry of image subsets, *Pattern Recogn. Lett.* **2** (1984) 311–317.

[12] A. Rosenfeld and A.C. Kak, *Digital Picture Processing, Vol.* 2, 2nd ed. (Academic Press, New York, 1982).

[13] E. Salari and P. Siy, The ridge-seeking method for obtaining the skeleton of digital images, *IEEE Trans. Systems Man Cybernet.* **14** (1984) 524–528.